NJC

New Journal of Chemistry

An international journal of the chemical sciences

www.rsc.org/njc

Volume 33 | Number 7 | July 2009 | Pages 1441–1620

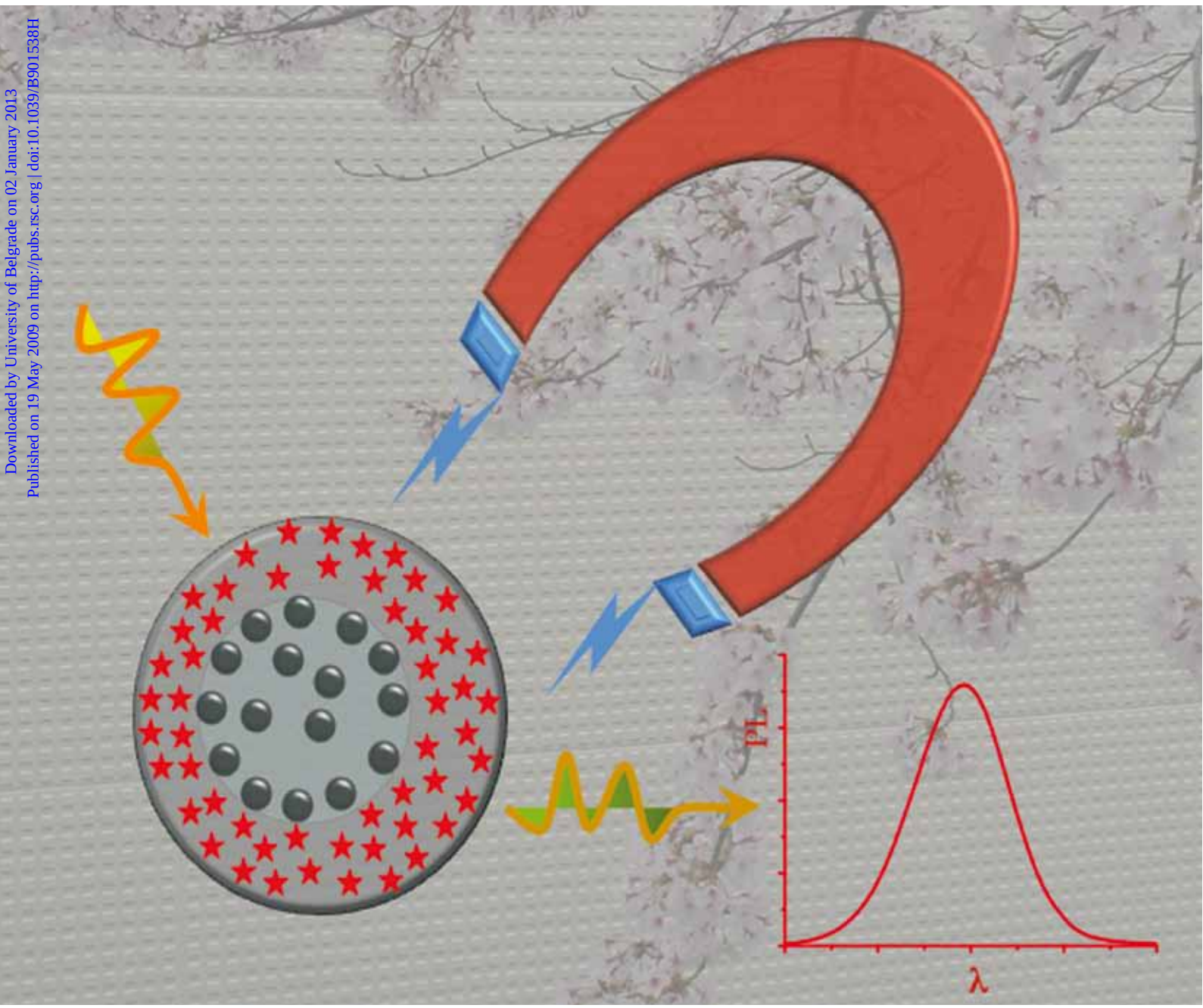

ISSN 1144-0546

RSC Publishing

LETTER

Norio Murase *et al.*

Preparation of SiO_2 beads with highly luminescent and magnetic nanocrystals *via* a modified reverse micelle process

Preparation of SiO_2 beads with highly luminescent and magnetic nanocrystals *via* a modified reverse micelle process

Ping Yang, Masanori Ando and Norio Murase*

Received (in Montpellier, France) 23rd January 2009, Accepted 28th April 2009
First published as an Advance Article on the web 19th May 2009
DOI: 10.1039/b901538h

Sol–gel-derived SiO_2 beads (100–200 nm) encapsulating highly luminescent semiconductor nanocrystals can additionally host other materials, such as magnetic nanocrystals, in a specially prepared hollow within the bead so as to achieve dual functionality.

Magnetic nanocrystals (NCs) have been used for magnetic resonance imaging, drug delivery, cell labeling and magnetic cell separation.[1] Photoluminescence (PL) has become one of the most studied functionalities of magnetic systems, because luminescent and magnetic properties are advantageous when combined for applications in biodetection, biosensing, bioseparation and targeted drug delivery.[2] Because ideal luminescent probes should emit at spectroscopically resolvable energies, have a narrow, symmetric emission spectrum, and because whole groups of probes should be excitable at a single wavelength, semiconductor NCs for biolabeling have opened up new possibilities compared to conventional dye molecules. SiO_2 beads are attractive candidates as containers for biomedical and environmental research applications because of their biocompatibility and stability against degradation. Furthermore, the surface of SiO_2 beads can be easily modified with a wide range of functional groups. Multiple types of functional SiO_2 beads have thus been widely applied after surface modification in biomedical and biopharmaceutical fields.[3] For example, Rosenzweig *et al.* prepared luminescent SiO_2 beads with sizes of several tens to several hundreds of nanometers for bioanalytical assays.[3e] Legrand and co-workers have also reported luminescent SiO_2 beads with a mean size of 200 nm for biomedical applications.[3f] Very few papers have been published on SiO_2 beads with dual functionality to date, even though such beads have been an important research topic for medical and biological applications.

Hitherto, several sol–gel approaches have been used to synthesize magnetic-luminescent SiO_2 beads, as shown in Scheme 1.[3] The direct attachment of magnetic and LNCs during long complicated synthesis procedures, however, decreases the PL efficiency of the resulting NCs. PL efficiency in the context of this Letter is the quantum efficiency defined by the probability of photon emission when excited. For example, a three-fold decrease in the PL efficiency has been reported for magnetic-LNCs (Fe_2O_3 core with a shell of CdSe/ZnS NCs).[4] A PL efficiency of about 15% was reported for γ-Fe_2O_3/QD605 (CdSe/ZnS NCs, commercial) micelles containing a 1 : 1 molar ratio of magnetic and fluorescent particles, whereas the initial efficiency of the QD605 measured in $CHCl_3$ was 41%.[5] Therefore, it is necessary to develop a novel preparation procedure for encapsulating these two kinds of NCs into SiO_2 beads without degrading the initially high PL efficiency.

There are two sol–gel methods for the preparation of SiO_2 beads in the literature: Stöber synthesis and reverse micelle synthesis.[3] We have prepared SiO_2 beads with highly luminescent CdTe or ZnSe NCs by a reverse micelle synthesis process after pre-treatment by the Stöber process.[6] The CdTe NCs retained their initial PL efficiency (65%) in the resulting SiO_2 beads.[6b] The synthesis conditions affecting the hydrolysis and condensation reactions of silicon alkoxides ($Si(OR)_4$) have been well studied. We obtained two types (hollow and egg yolk structure) of SiO_2 beads with CdTe NCs by controlling the sol–gel processes.[6d] These beads achieved a PL efficiency of 70% after being re-dispersed in pure H_2O. In this Letter, we present our current progress in developing single SiO_2 beads with multiple Fe_3O_4 and CdTe NCs by using both the Stöber and reverse micelle processes. Instead of adding the aqueous phase all at once, as previously carried out for reverse micelle methods, we added an aqueous solution of thin SiO_2-coated CdTe NCs (first aqueous phase), prepared by the Stöber process, at the beginning of the reverse micelle process. When an aqueous solution of Fe_3O_4 NCs (second aqueous phase) was subsequently added after moderate condensation of the hydrolyzed silicon alkoxide from the first aqueous phase, the Fe_3O_4 NCs were incorporated into the hollow spaces created by the second aqueous phase in the beads, separate from the

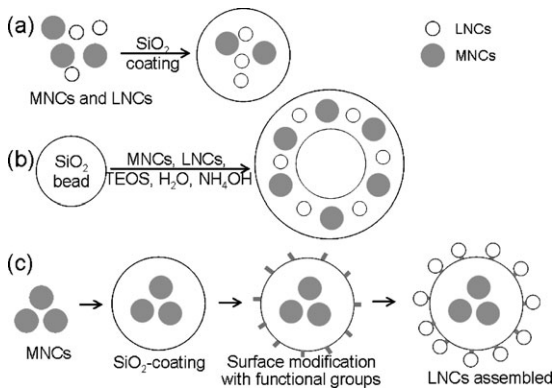

Scheme 1 The existing synthesis procedures for SiO_2 beads with magnetic nanocrystals (MNCs) and luminescent nanocrystals (LNCs).

Photonics Research Institute, National Institute of Advanced Industrial Science and Technology, Midorigaoka, Ikeda City, Osaka 563-8577, Japan. E-mail: n-murase@aist.go.jp

CdTe NCs. This two-step aqueous phase addition resulted in a high PL efficiency (68%) for the CdTe NCs in the SiO_2 beads. Scheme 2 shows this preparation and formation process. As explained later, the second aqueous phase contained Fe_3O_4 NCs, with the higher pH playing an important role in maintaining the high PL efficiency of the CdTe NCs.

Fig. 1(a–c) show transmission electron microscopy (TEM) photographs of the prepared SiO_2 beads (one specimen at different positions). The mean size of the Fe_3O_4 NCs used for the preparation was 8 nm, as shown in Fig. 1(d). The beads shown in Fig. 1(a) and (b) exhibit a hollow structure. Fig. 1(c) clearly shows the CdTe NCs (mean size ~4 nm) dispersed in the solid part and the Fe_3O_4 NCs (larger black dot) dispersed in the middle part of a bead. The histogram shown in Fig. 1(e) was plotted by measuring the sizes of hundreds of beads in the TEM pictures. For comparison, a TEM picture of hollow SiO_2 beads is shown in Fig. 1(f). As we explained in a previous paper,[6d] these empty beads only contained CdTe NCs in the SiO_2 matrix. Therefore, no dark area was observed in their middle parts. For bead preparation, the reaction time for step 1 in Scheme 2 was 2 h. Because no ethanol was added during step 1, the tetraethyl orthosilicate (TEOS) was only partially hydrolyzed. When the second aqueous phase was added in step 2, the newly formed small droplets were encapsulated in the droplets created by the previous addition

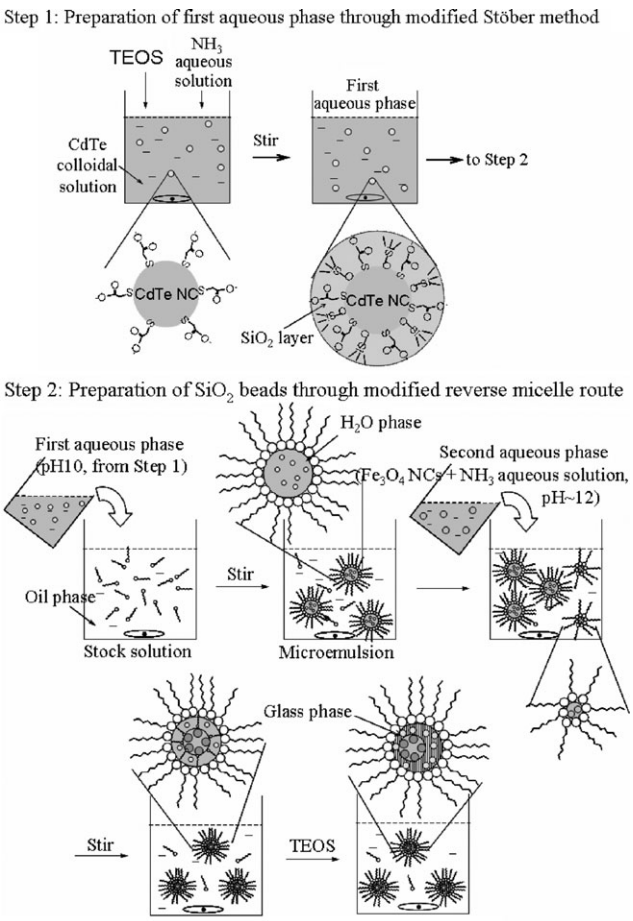

Scheme 2 The preparation and formation process for SiO_2 beads encapsulating CdTe and Fe_3O_4 NCs by a two-step synthesis.

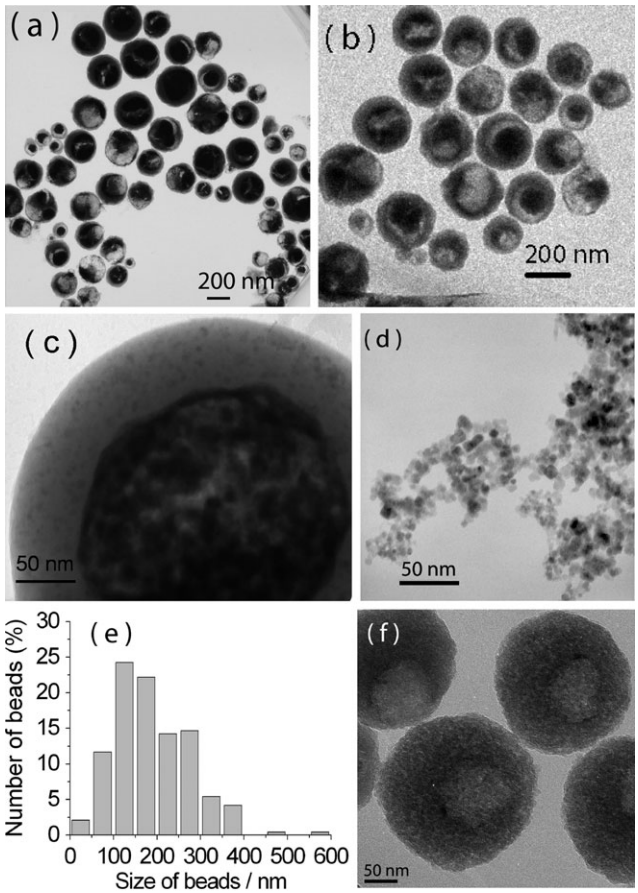

Fig. 1 (a–c) TEM photographs of SiO_2 beads encapsulating Fe_3O_4 and CdTe NCs. (d) A TEM photograph of Fe_3O_4 NCs before encapsulation. Picture (c) shows that the Fe_3O_4 NCs are located in the middle part of the beads, while the CdTe NCs are dispersed within the solid part of the bead (SiO_2 shell). Because of the high magnification, the originally hollow part in (c) was modified by the focused electron beam (300 KeV, *ca.* 8 μA) during the observation. (e) The size distribution of the beads. The histogram was plotted by measuring the size of hundreds of beads in TEM photographs. (f) A TEM picture of hollow SiO_2 beads is shown for comparison.

of the first aqueous phase. Since the pH of the second aqueous phase (ammonia solution dispersing Fe_3O_4 NCs, with a pH of 12) was higher than that of the first aqueous phase (precursor solution after step 1, with a pH of 10), condensation of the SiO_2 sol at the interface between the two aqueous phases occurred quickly when the second aqueous phase entered the first. This created an SiO_2 wall on the surface of the second aqueous phase in the droplet of the first aqueous phase. This wall played two roles in the formation of SiO_2 beads. The first was as a barrier to separate the two kinds of NCs, while the second is was as a template to form a hollow structure. Since the second aqueous phase does not contain alkoxide, this component creates the hollow part. Because the Fe_3O_4 NCs are positively charged and the SiO_2 gel is negatively charged, the NCs attached to the SiO_2 wall created at the interface with the second aqueous phase. Furthermore, the remaining NCs in the second aqueous phase were subsequently deposited after the H_2O in the hollow part was removed during the separation process for the beads.

Therefore, dark areas, consisting of many Fe_3O_4 NCs in the middle parts of the beads, were observed in the TEM photographs.

Fig. 2 shows the powder X-ray diffraction (XRD) pattern of the as-prepared beads. The positions of six diffraction peaks match well with the cubic spinel structure of magnetite. Three other diffraction peaks are indexed to cubic CdTe. A vibrating sample magnetometer (VSM) measurement shows of both the beads and the pure Fe_3O_4 NCs superparamagnetic behavior (Fig. 3) at room temperature. The magnetic saturation values of the Fe_3O_4 NCs and as-prepared beads were 44 and 3 emu g^{-1}, respectively. The difference in the saturation value is mainly due to the weight fraction of the Fe_3O_4 in the beads.

To further clarify that the two kinds of NCs exist separately in these beads, we employed annular dark-field scanning transmission electron microscopy (ADF-STEM) and energy-dispersive X-ray (EDX) analysis for characterization. Fig. 4 shows an ADF-STEM photograph of an SiO_2 bead (a) and the EDX analysis results ((b) and (c)) obtained from the indicated detection area of the SiO_2 bead. The EDX analyses indicated that the bead contains Cd, Te and Fe in its middle part. Cd and Te signals came from the SiO_2 shell on both sides of the detection area. Si, Cd and Te were detected in the solid part (SiO_2 shell) of the bead. This means that the Fe_3O_4 NCs are dispersed only in the middle part of the bead. Typical EDX analysis patterns with Fe (b) and without Fe (c) are shown in lower part of Fig. 4. In addition, a wet chemical analysis of these beads indicated a molar ratio for Si : Fe : Cd : Te : S of 1 : 0.017 : 0.027 : 0.011 : 0.017. The molar ratio of Cd : (Te + S) (= 1 : 1.04) in the beads is very similar to that of the initial red-emitting CdTe NCs (= 1 : 1.06) determined by inductively coupled plasma (ICP) analysis on this occasion. This means that capping agent thioglycolic acid (TGA) was retained on the surface of the NCs during preparation. Because the mean size of the Fe_3O_4 NCs was 8 nm, the number of Fe_3O_4 NCs in a bead (200 nm), whose hollow part has a size of 100 nm, was derived as being about 100 by simple calculation. According to our previous results, a green-emitting CdTe NC (2.6 nm in diameter) contains 70 Te ions.[8] This gives 210 Te ions for a red-emitting CdTe NC (3.9 nm in diameter). Therefore, the

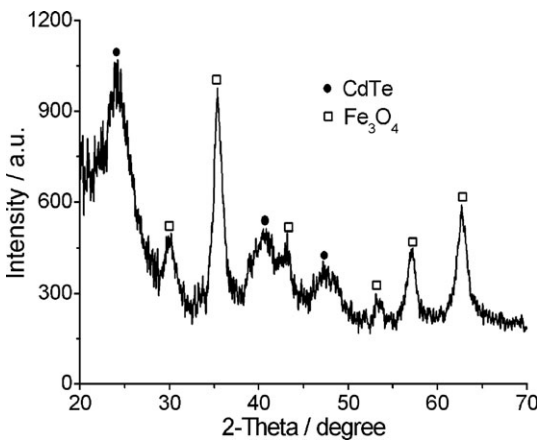

Fig. 2 The XRD pattern of the as-prepared beads. All of the diffraction peaks were indexed to cubic Fe_3O_4 or CdTe.

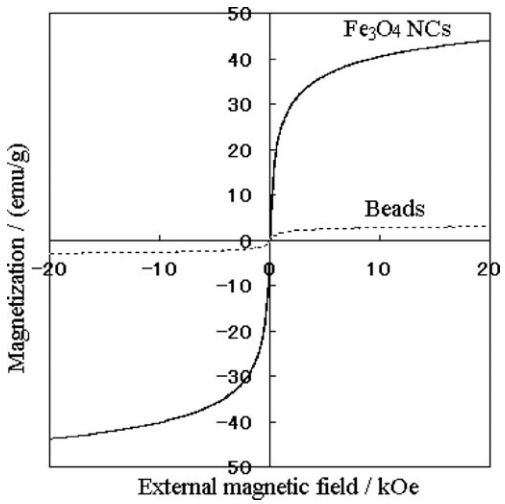

Fig. 3 Field-dependent magnetization plots of Fe_3O_4 NCs and as-prepared SiO_2 beads. The magnetic saturation values of the Fe_3O_4 NCs and the beads are 44 and 3 emu g^{-1}, respectively. The samples were measured after fixing with glue.

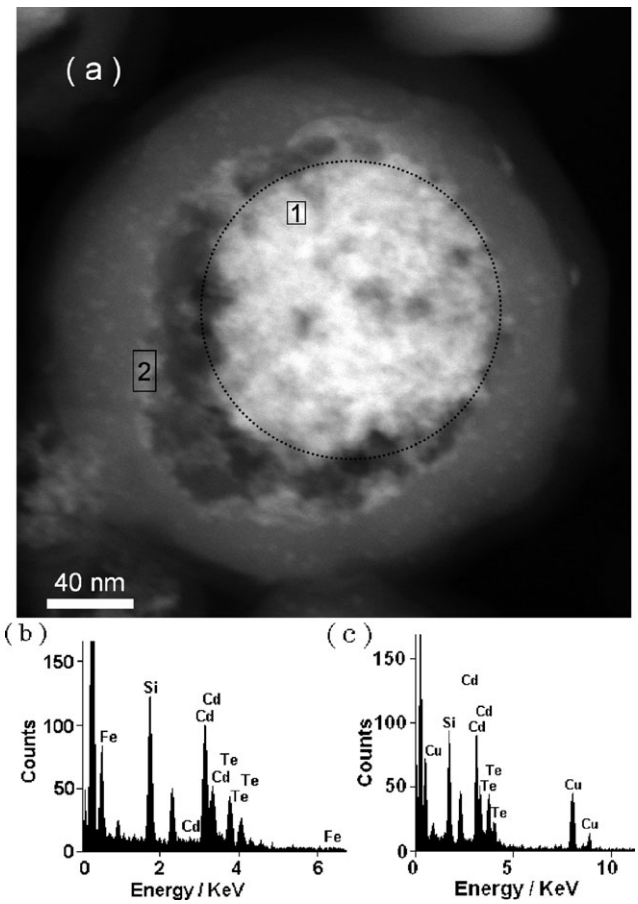

Fig. 4 (a) ADF-STEM photograph of a luminescent hollow SiO_2 bead encapsulating Fe_3O_4 NCs. (b) EDX data from area 1 in Fig. 4(a); an Fe signal was detected. (c) EDX data from area 2 in Fig. 4(a); an Fe signal was not detected. An Fe signal was detected only within the area shown by the black dotted circle.

average concentration of these NCs in the beads is estimated to be about 0.0017 M. In this case, there would be about

3700 CdTe NCs in a bead, with a diameter of 200 nm and a hollow part with a size of 100 nm.

Because the PL efficiency is crucially important for applications, we measured the PL properties of these beads. Fig. 5 shows the absorption and PL spectra of luminescent SiO_2 beads encapsulating Fe_3O_4 NCs (black line). The absorption and PL spectra of the initial CdTe colloidal solution are shown for comparison (grey line). A PL efficiency of 68% and a slight blue shift of the PL peaks were observed, whereas the PL efficiency of the initial CdTe colloidal solution was 71%. Since the absorbance of the beads was close to that of the CdTe NCs across the whole wavelength range in Fig. 5(a), the scattering component of the beads is small. Therefore, we concluded that the measured PL efficiency of the beads is reliable. To the best of our knowledge, this PL efficiency of 68% is the highest reported value for two kinds of NCs in SiO_2 beads. There have also been a few reports on the PL efficiency of SiO_2 beads with magnetic and LNCs. Ying *et al.* reported a PL efficiency of 4.8% for small SiO_2 beads ($\sim$50 nm) with magnetic and CdSe/ZnS NCs.[3c] They also prepared SiO_2 beads with connected Fe_3O_4–CdSe NCs (NCs with a very thin SiO_2 layer, several nanometers in total diameter), whose PL efficiency before and after SiO_2 coating was 13–18 and 8–10%, respectively.[9] These values are higher than the PL efficiency of 3.2% reported for FePt–CdS NCs.[10] Lai and colleagues prepared iridium complex-functionalized Fe_3O_4/SiO_2 core–shell beads ($\sim$50 nm), retaining a PL efficiency of 10%.[11] Guo *et al.* reported SiO_2-coated Fe_3O_4/SiO_2/CdTe beads ($\sim$160 nm).[12] In this case, the efficiency of the initial colloidal TGA-capped CdTe NCs was estimated to be 30–40%. They did not, however, indicate the PL efficiency of these beads. In contrast, our present approach, using the formation of a hollow structure, offers tremendous potential for maintaining the initial PL properties of NCs.

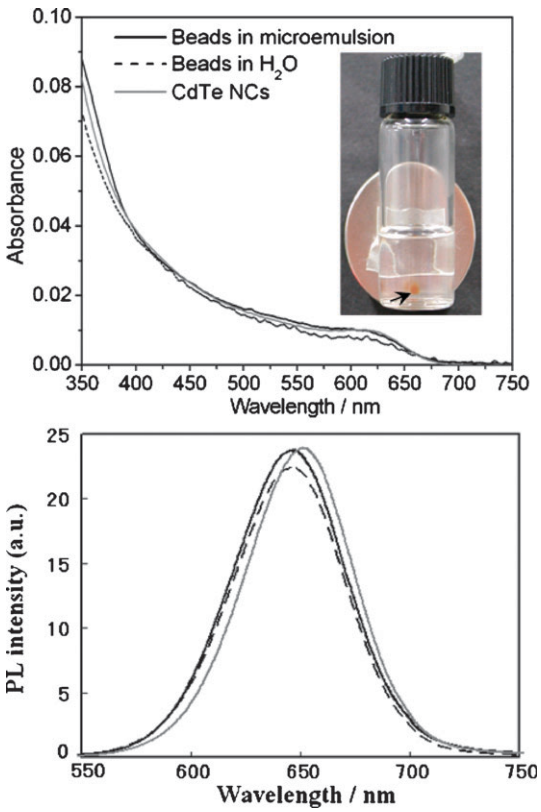

Fig. 5 Absorption (upper part) and PL (lower part) spectra of luminescent SiO_2 beads encapsulating Fe_3O_4 NCs in a microemulsion (black line, their size distribution is shown in Fig. 1(e)) and in H_2O (dashed black line, less than 200 nm in diameter). The beads were easily collected with a permanent magnet (insert, black arrow). The surface flux density of the magnet was 0.45 T. The absorption and PL spectra of a CdTe colloidal solution are shown for comparison (grey line). The PL efficiency of the beads in the microemulsion was 68%, while that of the CdTe colloidal solution was 71%. After re-dispersion in pure H_2O, the beads (less than 200 nm in diameter) revealed a PL efficiency of 40%.

There are two reasons why the CdTe NCs mostly retained their initial PL efficiency in our case. One was the thin SiO_2 shell coated onto the CdTe NCs before the reverse micelle process. This caused the NCs to retain the capping agent TGA on their surface after step 1. The thin SiO_2 shell then protected the NCs from the surrounding environment during the subsequent reverse micelle synthesis. The second reason was the addition of the second aqueous phase with a higher pH than that of the first aqueous phase. This resulted in rapid condensation of the SiO_2 sol at the interface in the beads after their incorporation into H_2O droplets. This SiO_2 wall hindered the attachment of the two kinds of NCs during the preparation.

For further applications, we separated the beads from the microemulsion by filtering and centrifugation. After filtering again with a 0.2 μm filter and washing the beads three times with ethanol, they were collected with a permanent magnet in order to remove them without impregnating the magnetic NCs. Next, the beads were washed with H_2O and re-dispersed in H_2O for further characterization. The absorption and PL spectra of the beads in H_2O are also shown in Fig. 5 as dashed black lines. The insert in Fig. 5 shows how the beads were collected using the magnet. After re-dispersion of the beads in pure H_2O, their PL efficiency decreased to 40%. This value is still the highest among the reported values in the literature for SiO_2 beads with luminescent and magnetic NCs in pure H_2O. This decrease in PL efficiency is attributed to the complicated separation process, which results in surface deterioration of the CdTe NCs.

In conclusion, hollow SiO_2 beads encapsulating CdTe and Fe_3O_4 NCs were prepared by a two-step sol–gel synthesis, consisting of a modified Stöber synthesis and a subsequent reverse micelle process. The SiO_2 beads exhibited a high PL efficiency of 68%. Because the beads revealed a similar magnetic behavior to that of pure Fe_3O_4 NCs and because of their high PL efficiency, we will next focus on their bio-applications, such as magnetic resonance imaging, drug delivery, cell labeling and magnetic cell separation. In addition, the proposed process should open up a new approach for preparing SiO_2 beads with dual functions by dispersing other materials in their hollow part, such as metal NCs, oxide NCs and dye molecules.

This study was supported in part by the Creation and Support Program for Start-Ups from Universities, sponsored by the Japan Science and Technology Agency (JST). P. Y. is

also grateful for a Research Fellowship from the Japan Society for the Promotion of Science (JSPS).

Experimental section

Preparation of two kinds of NCs

TGA-capped CdTe NCs (red-emitting) in an aqueous solution were prepared by a procedure using cadmium perchlorate and hydrogen telluride, as described in a previous paper.[13]

Magnetite (Fe_3O_4) NCs in an aqueous solution without any surfactants were obtained as described in the literature.[7] Briefly, 0.10 mL of 12 M HCl and 5 mL of purified deoxygenated H_2O (obtained by nitrogen gas bubbling for 30 min) were mixed, and 0.1038 g of $FeCl_2$ and 0.26 g of $FeCl_3$ were successively dissolved in the solution by stirring. The resulting solution was added dropwise into 25 mL of a 1.5 M NaOH solution under vigorous stirring. The precipitate was isolated with a magnet and the supernatant was removed from the precipitate by decantation. Purified deoxygenated H_2O was then added to the precipitate, and the solution was decanted after centrifugation at 4000 rpm. After repeating this latter procedure three times, 50 mL of 0.01 M HCl solution was added to the precipitate (with stirring) to neutralize the anionic charges on the NCs. The sample was again separated by centrifugation (4000 rpm) and peptized by adding H_2O.

Preparation of beads

SiO_2 beads containing CdTe and Fe_3O_4 NCs were prepared by a two-step synthesis process, as follows: (1) the LNCs were coated with a thin SiO_2 layer and (2) these SiO_2-coated NCs were encapsulated into SiO_2 beads, together with Fe_3O_4 NCs. The details of each step are given below.

Step 1: The CdTe NCs were re-dispersed into an aqueous solution of Cd^{2+} ($Cd(ClO_4)_2{\cdot}H_2O$) and TGA, after adjusting the molar ratio (such as 1 : 3) of Cd : TGA and their concentrations (0.0025 M TGA). The pH of the solution of Cd^{2+} and TGA was kept at 10 using an NaOH solution. The re-dispersed CdTe colloidal solution (2 mL, 2.2×10^{-6} M), a diluted ammonia solution (50 μL, 6.25 wt%) and TEOS (20 μL) were mixed in a covered vial for 2 h to obtain the first aqueous phase of CdTe NCs coated with a thin SiO_2 layer by a modified Stöber synthesis process.

Step 2: To obtain the stock solution, Igepal CO-520 (3.52 g) was added to cyclohexane (25 g) whilst stirring until the solution became clear. To prepare the microemulsion, the first aqueous phase (~2 mL) was initially injected through a reverse micelle method into the stock solution drop by drop whilst vigorously stirring. An ammonia solution of Fe_3O_4 NCs (pH ~ 12, 100 μL) (second aqueous phase) was then injected dropwise. The reaction time for step 2 was normally 24 h.

Apparatus

The observations by TEM and ADF-STEM and analysis by EDX were carried out on Hitachi H-9000NA (300 kV) or FEI Tecnai G2 F20 (200 kV) electron microscopes. The XRD pattern of a sample was obtained using an X-ray diffractometer (Rigaku, Geigerflex). The molar ratio of Te : Cd : Si : Fe in the beads was measured with an inductively coupled plasma spectrometer after dissolving them in acid (SPS4000, SII Nanotechnology Inc.). The magnetic properties were recorded by using a vibrating sample magnetometer (BHV-525, Riken Denshi Co. Ltd.). The absorption and PL spectra were collected using conventional spectrometers (Hitachi U-4000 and F-4500). The PL efficiencies of the emitting beads and CdTe NCs in solution were estimated by a method we reported previously,[14] where quinine in 0.1 N sulfuric acid solution (55%) was used as a standard. The excitation wavelength was set to 365 nm.

References

1 Y. Jun, Y. M. Huh, J. Choi, J. H. Lee, H. T. Song, S. Kim, S. Yoon, K. S. Kim, J. S. Shin, J. S. Suh and J. Cheon, *J. Am. Chem. Soc.*, 2005, **127**, 5732; Y. M. Huh, Y. Jun, H. Soog, S. Kim, J. Choi, J. Lee, S. Yoon, K. Kim, J. Shin, J. Suh and J. Cheon, *J. Am. Chem. Soc.*, 2005, **127**, 12387.
2 V. Salgueiriño-Maceira and M. A. Correa-Duarte, *Adv. Mater.*, 2007, **19**, 4131.
3 (*a*) N. Insin, J. B. Tracy, H. Lee, J. P. Zimmer, R. M. Westervelt and M. G. Bawendi, *ACS Nano*, 2008, **2**, 197; (*b*) M. Li, Z. Chen, V. W.-W. Yam and Y. Zu, *ACS Nano*, 2008, **2**, 905; (*c*) D. K. Yi, S. T. Selvan, S. S. Lee, G. C. Papaefthymiou, D. Kundaliya and J. Y. Ying, *J. Am. Chem. Soc.*, 2005, **127**, 4990; (*d*) Y. Zhang, S. Pan, X. Teng, Y. Luo and G. Li, *J. Phys. Chem. C*, 2008, **112**, 9623; (*e*) L. M. Rossi, L. Shi, F. H. Quina and Z. Rosenzweig, *Langmuir*, 2005, **21**, 4277; (*f*) S. Legrand, A. Catheline, L. Kind, E. C. Constable, C. E. Housecroft, L. Landmann, P. Banse, U. Pieles and A. Wirth-Heller, *New J. Chem.*, 2008, **32**, 588.
4 D. Wang, J. He, N. Rosenzweig and Z. Rosenzweig, *Nano Lett.*, 2004, **4**, 409.
5 V. Roullier, F. Grasset, F. Boulmedais, F. Artzner, O. Cador and V. Marchi-Artzner, *Chem. Mater.*, 2008, **20**, 6657.
6 (*a*) S. T. Selvan, C. L. Li, M. Ando and N. Murase, *Chem. Lett.*, 2004, **33**, 434; (*b*) P. Yang, M. Ando and N. Murase, *J. Colloid Interface Sci.*, 2007, **316**, 420; (*c*) M. Ando, C. L. Li, P. Yang and N. Murase, *J. Biomed. Biotechnol.*, 2007, 52971; (*d*) P. Yang, M. Ando and N. Murase, *New J. Chem.*, 2009, **33**, 561.
7 Y. S. Kang, S. Risbud, J. F. Rabolt and P. Stroeve, *Chem. Mater.*, 1996, **8**, 2209.
8 N. Murase, N. Gaponik and H. Weller, *Nanoscale Res. Lett.*, 2007, **2**, 230.
9 S. T. Selvan, P. K. Patra, C. Y. Ang and J. Y. Ying, *Angew. Chem., Int. Ed.*, 2007, **46**, 2448.
10 H. Gu, R. Zheng, X. X. Zhang and B. Xu, *J. Am. Chem. Soc.*, 2004, **126**, 5664.
11 C. Lai, Y. Wang, C. Lai, M. Yang, C. Chen, P. Chou, C. Chan, Y. Chi, Y. Chen and J. Hsiao, *Small*, 2008, **4**, 218.
12 J. Guo, W. Yang, C. Wang, J. He and J. Chen, *Chem. Mater.*, 2006, **18**, 5554.
13 C. Li and N. Murase, *Chem. Lett.*, 2005, **34**, 92.
14 N. Murase and C. L. Li, *J. Lumin.*, 2008, **128**, 1896.